Supporting Information

Highly Efficient Blackberry-like Trimetallic PdAuCu Nanoparticles with Optimized Pd Content for Ethanol Electrooxidation

Yinyin Liang,[a†] Tao Ma,[a†] Yazhou Xiong,[a] Lizhu Qiu,[a] Hui Yu,[b] and Feng Liang*[a]

[a] The State Key Laboratory of Refractories and Metallurgy, School of Chemistry and Chemical Engineering, Wuhan University of Science and Technology, Wuhan 430081, P. R. China.

[b] Department of Civil and Environmental Engineering, Temple University, Philadelphia, PA 19122, USA

*E-mail: feng_liang@whu.edu.cn

†These authors contributed equally to this work.

Contents

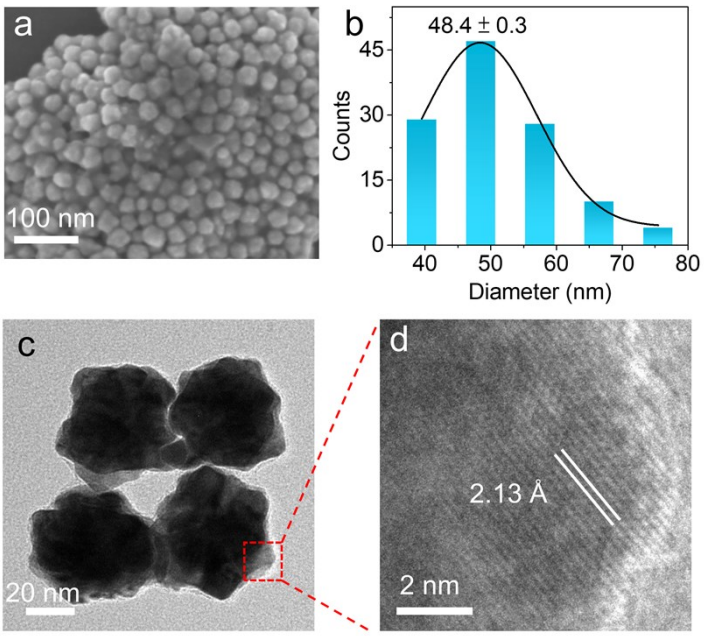

Fig. S1 (a) SEM image, (b) size distribution and (c) high-magnification TEM image of PdAuCu NPs-1, (d) corresponding HRTEM image in (c).

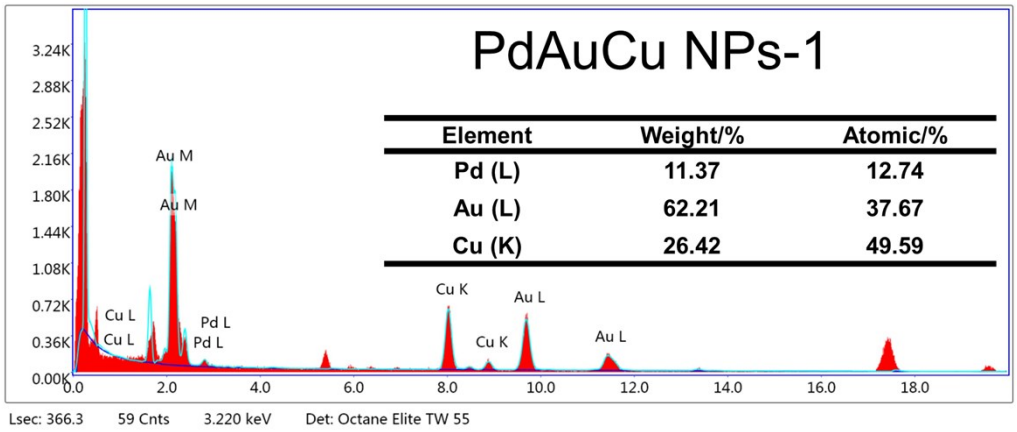

Fig. S2 EDX spectra of trimetallic PdAuCu NPs -1 and the table of corresponding element content of Pd, Au and Cu (inset).

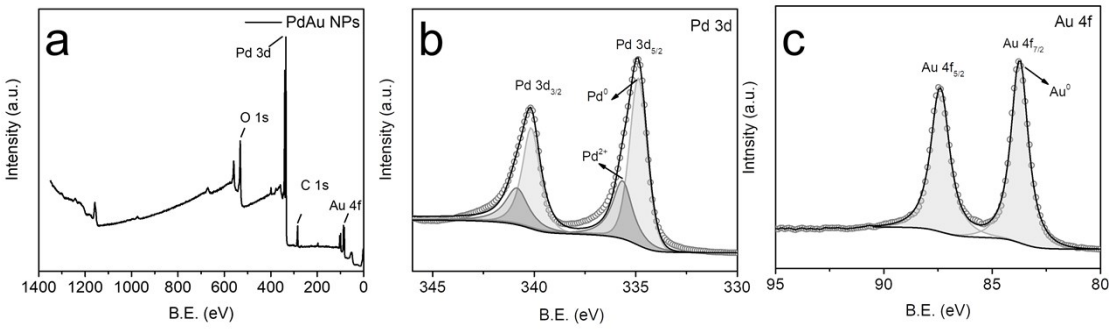

Fig. S3 (a) XPS survey spectra, (b) high-resolution Pd 3d and (c) Au 4f XPS spectra of PdAu NPs, the ratio of Pd^0/Pd^{2+} is 0.89.

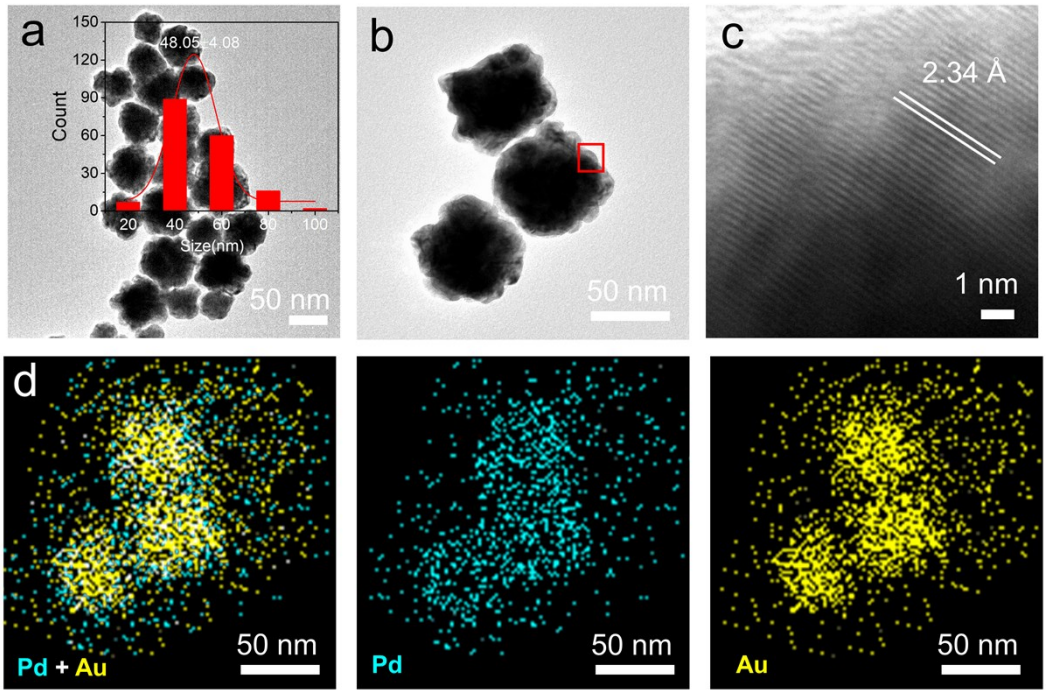

Fig. S4 (a) Low-magnification TEM image and corresponding size distributions (inset), (b) Low-magnification TEM image, (c) HRTEM image of red area in (b) and (d) the corresponding EDX mapping of PdAu NPs.

The morphology of PdAu NPs is similar to that of PdAuCu NPs-1, with a flower-like shape and a particle size of about 48 nm. And the lattice fringe is about 2.34 Å, which corresponds to the plane of (111) PdAu NPs alloy. Element mapping detected Pd and Au and they are evenly distributed over the nanoparticles, which further illustrated the alloy structure.

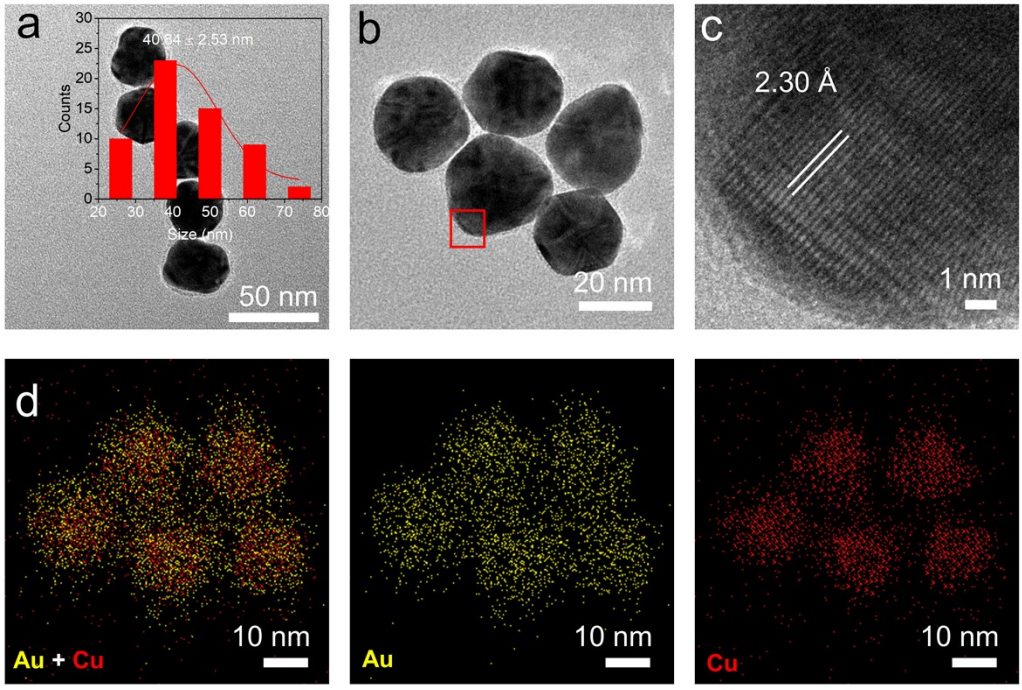

Fig. S5 (a) Low-magnification TEM image and corresponding size distributions (inset), (b) high-magnification TEM image , (c) HRTEM image of red area in (b) and (d) the corresponding EDX mapping of AuCu NPs.

The morphology of AuCu NPs is quasi-spherical with edges and corners and its size is about 40 nm. The lattice fringe of AuCu NPs with 2.30 Å, between that of Au(2.36Å) and Cu(2.08 Å), indicating Cu atoms incorporating into Au lattice, which illustrated the formation of the alloy structure. And the signal of Au and Cu were evenly distributed in the element mapping image, indicating that an alloy structure was formed.

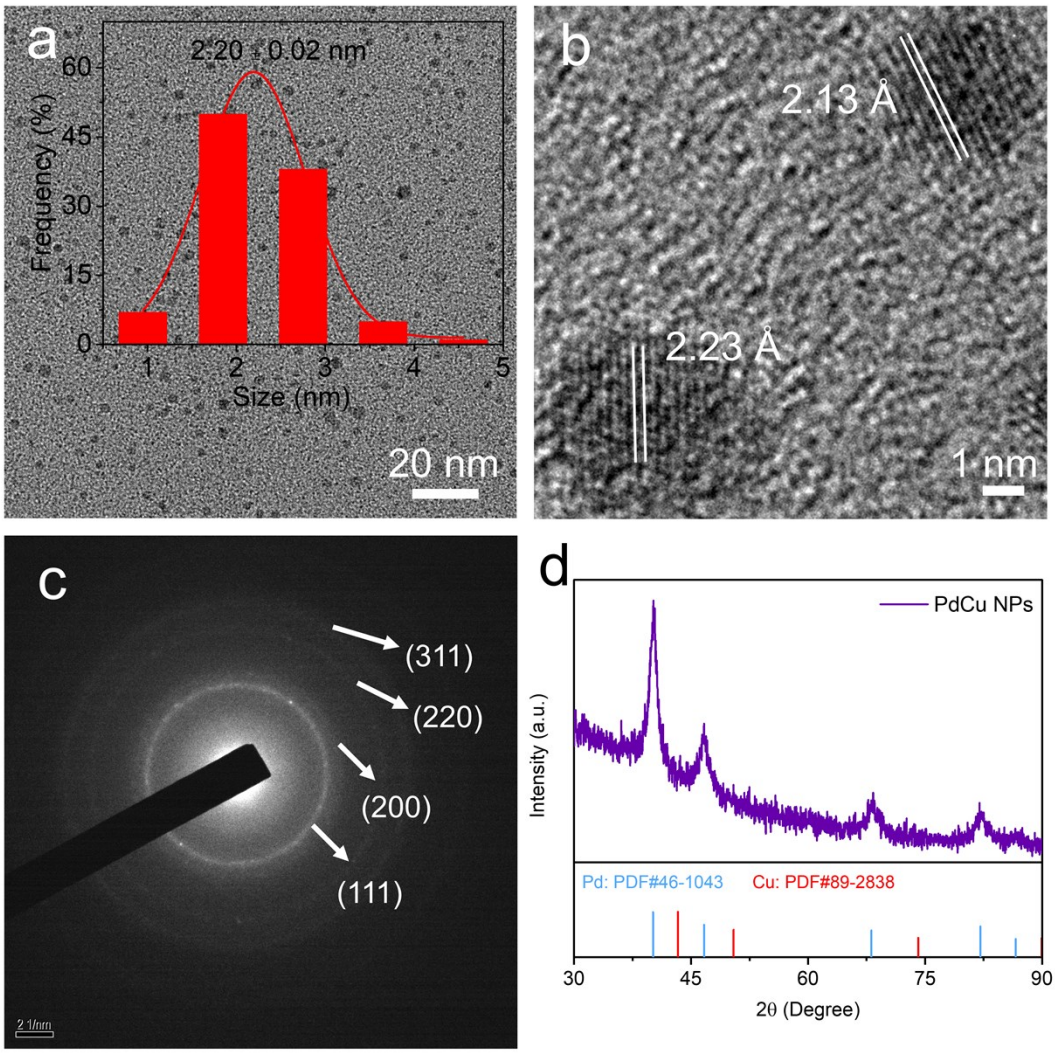

Fig. S6 (a) Low-magnification TEM image and corresponding size distributions (inset), (b) HRTEM image, (c) selected area electron diffraction (SAED) and (d) spectra of wide-angle XRD pattern of PdCu NPs.

The PdCu NPs were small size and spherical morphology. The lattice fringe of 2.13 Å and 2.23 Å were observed, which between Pd(2.24 Å) and Cu (2.08 Å) could be attributed to the (111) plane of PdCu NPs. The SAED image and XRD spectra clearly presented the planes of (111), (200), (220) and (311) revealing the alloy structure, and the XRD typical sharp diffraction peaks were shifted between Pd(PDF#46-1043) and Cu(PDF#89-2838), further confirmed the formation of bimetallic PdCu NPs.

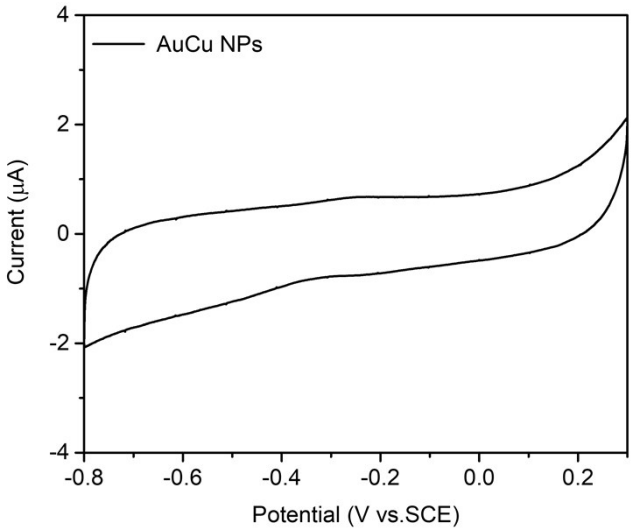

Fig. S7 CV curve of AuCu NPs in 1.0 M KOH and 1.0 M ethanol solution.

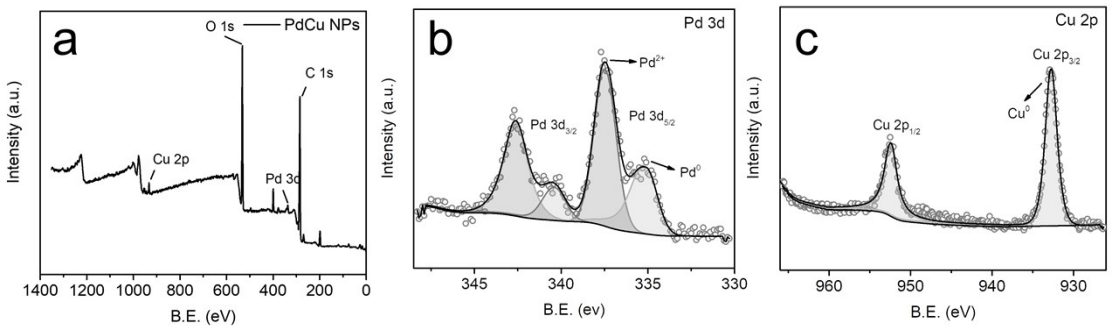

Fig. S8 (a) XPS survey spectra, (b) high-resolution Pd 3d and (c) Cu 2p XPS spectra of PdCu NPs, the ratio of Pd^0/Pd^{2+} is 0.48.

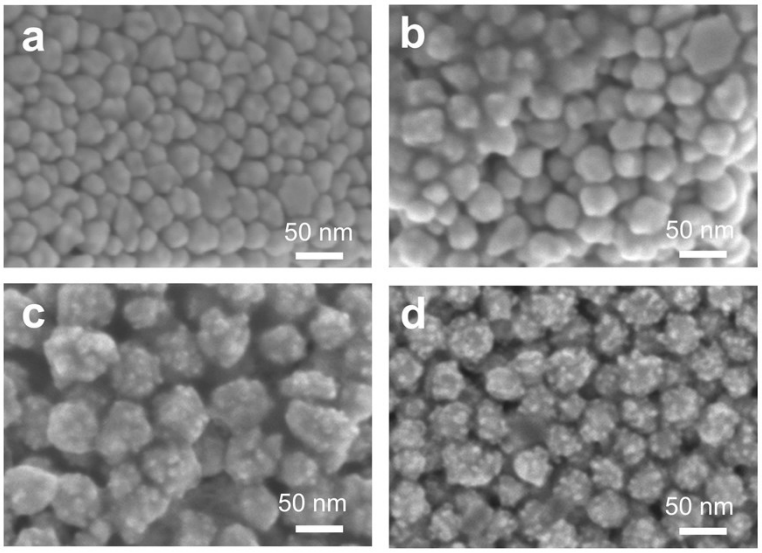

Fig. S9 SEM images of (a) PdAuCu NPs-0.1, (b) PdAuCu NPs-0.5, (c) PdAuCu NPs-2, and (d) PdAuCu NFs-3 NPs.

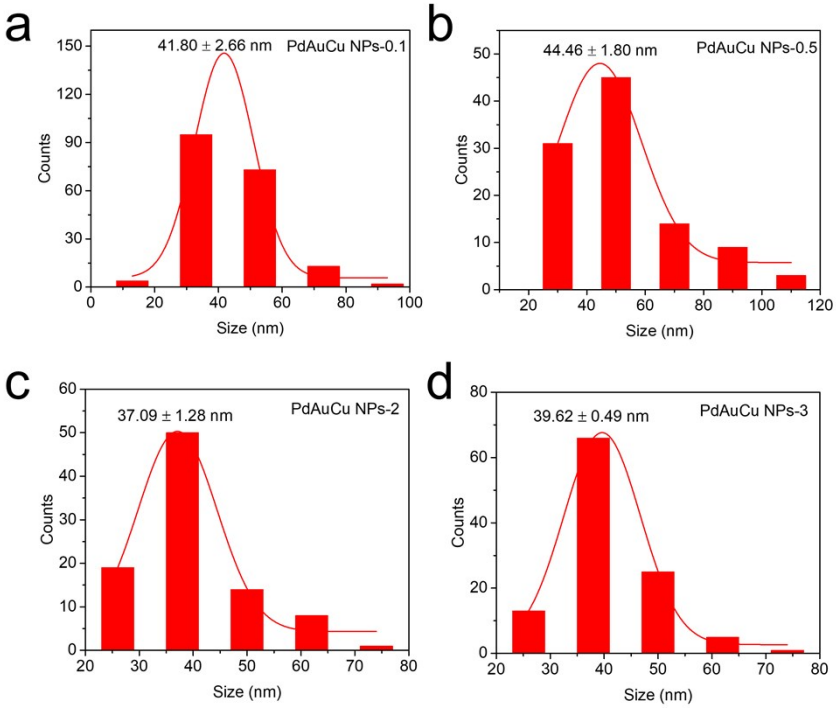

Fig. S10 The size distributions of (a) PdAuCu NPs-0.1, (b) PdAuCu NPs-0.5, (c) PdAuCu NPs-2, and (d) PdAuCu NPs-3

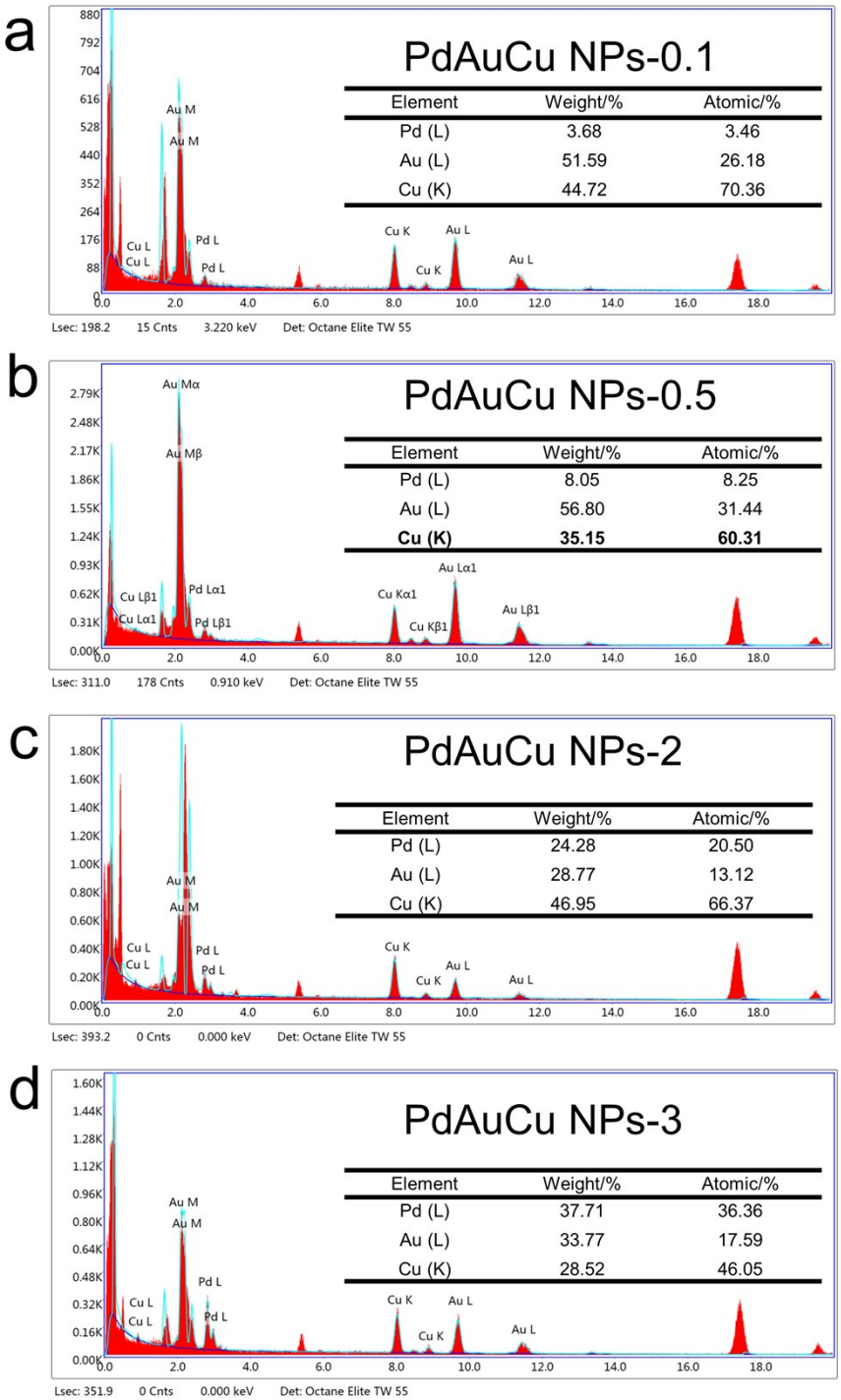

Fig. S11 EDX spectrum of (a) PdAuCu NPs-0.1, (b) PdAuCu NPs-0.5, (c) PdAuCu NPs-2, and (d) PdAuCu NPs-3, the table in each spectrum was the element content of Pd, Au and Cu.

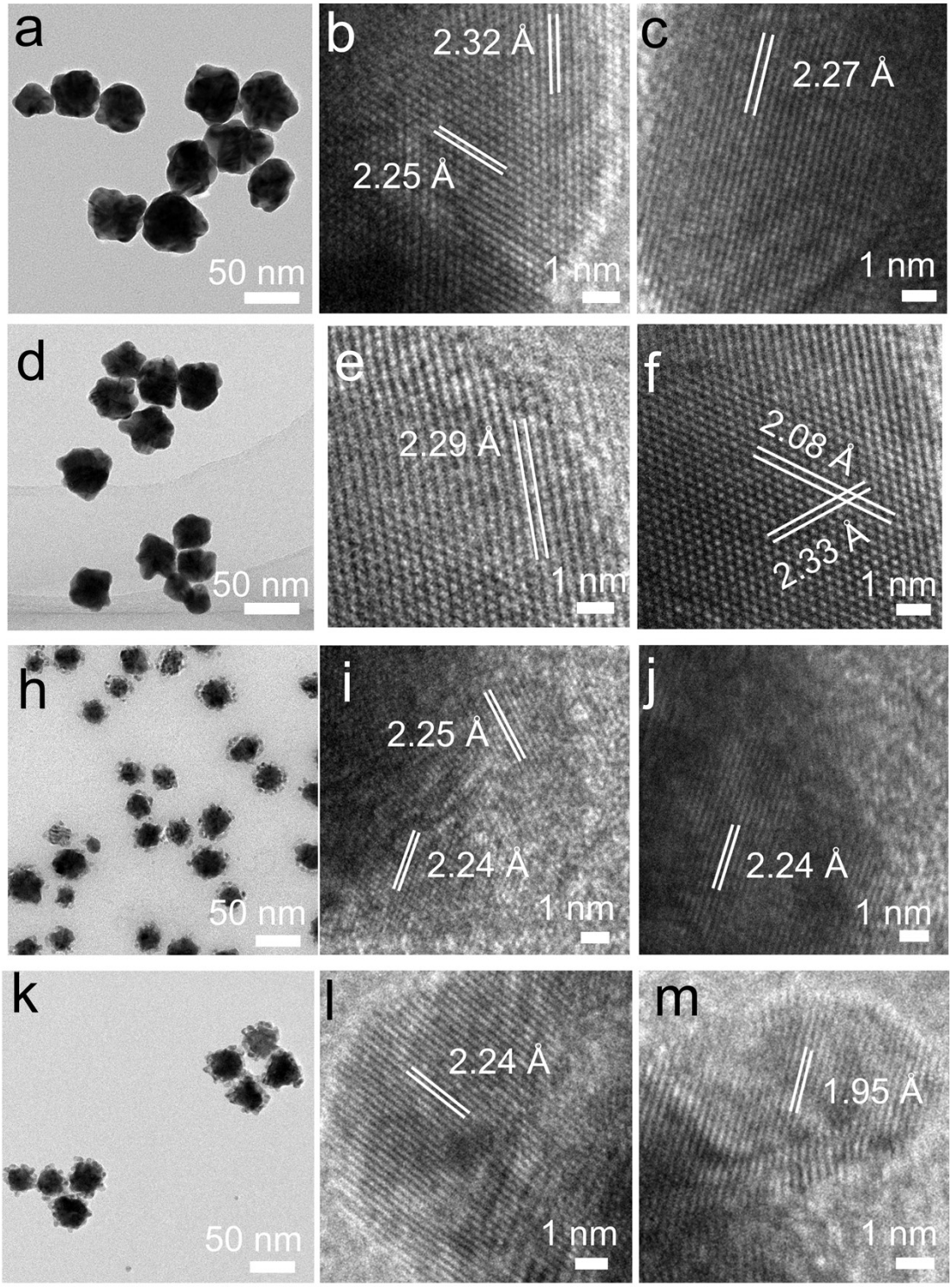

Fig. S12 Low-magnification (a, d, g and j) and high-magnification (b, c, e, f, h, I, k and l) TEM images of PdAuCu NPs-0.1 (a, b and c), PdAuCu NPs-0.5 (d, e and f), PdAuCu NPs-2 (g, h and i) and PdAuCu NPs-3 (j, k and l)

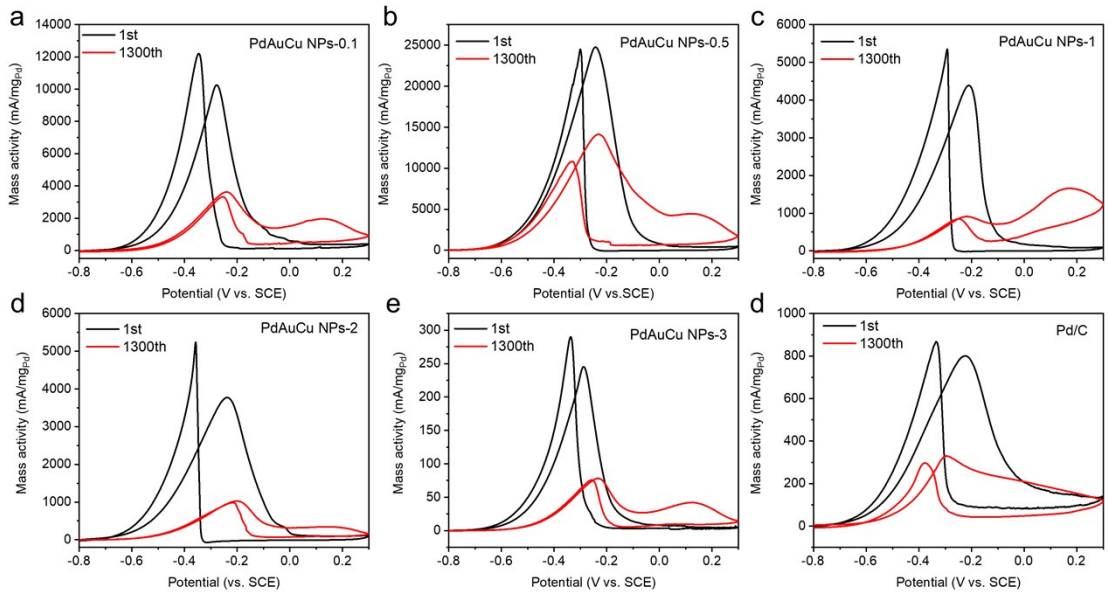

Fig. S13 The CVs before and after 1300 sweeps of (a) PdAuNPs-0.1, (b) PdAuNPs-0.1, (c) PdAuNPs-0.1, (d) PdAuNPs-0.1, (e) PdAuNPs-0.1, and (f) commercial Pd/C were recorded in 1 M KOH with 1.0 M ethanol solution at a scan rate of 50 mV/s.

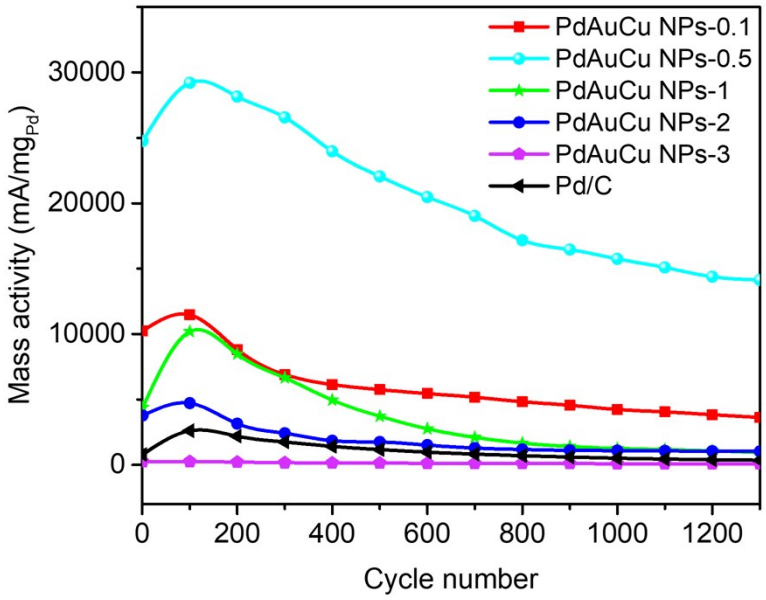

Fig. S14 The plots of forward peak current density from Fig. S13.

Table S1 Element content of as-prepared catalysts according to ICP-AES analysis.

Nanoparticles	Pd (mg/L)	Au (mg/L)	Cu (mg/L)	Pd (%)
PdAuCu NPs-0.1	26.2	1574	0.48	1.64
PdAuCu NPs-0.5	51.4	1981.6	2.2	2.52
PdAuCu NPs-1	133.4	1683.4	13.8	7.29
PdAuCu NPs-2	280	1313	26.8	17.29
PdAuCu NPs-3	345	1179.6	20.6	22.33
PdAu NPs	406.6	1691.8	-	19.38
PdCu NPs	62.4	-	68.5	47.67

Table S2 The ratio of Pd^0 and Pd^{2+} in trimetallic PdAuCu NFs-(0.1, 0.5, 1, 2 and 3) and bimetallic PdAu and PdCu NPs catalysts according to XPS analysis.

Nanoparticles	Pd^0 (At. %)	Pd^{2+} (At. %)	Pd^0/Pd^{2+}
PdAuCu NPs-0.1	100	0	-
PdAuCu NPs-0.5	66.46	33.64	1.98
PdAuCu NPs-1	67.94	32.06	2.12
PdAuCu NPs-2	68.93	31.07	2.22
PdAuCu NPs-3	76.77	23.23	3.30
PdAu NPs	47.16	52.84	0.89
PdCu NPs	32.62	67.38	0.48
Commercial Pd/C	21.59	78.41	0.28

Table S3 Comparison of the electrochemical performance of various Pd-based nanomaterials for EOR in alkaline media.

Catalyst	Electrolyte	Mass activity (mA/mg_{Pd})	ECSA (m^2/g_{Pd})	Stability	Ref.
PdAgCu	1.0 M KOH and 1.0 M ethanol	4640	49.8	NA	[1]
Au@PdAuCu	1.0 M KOH and 1.0 M ethanol	3990	41.2	1200 mA mg_{Pd}^{-1} after5000s	[2]
Au@AgPd	0.3M KOH and 0.50 M ethanol	1160	77.5	NA	[3]
PdPtCu	1.0 M KOH and 1.0 M ethanol	3790	46.3	1310 mA mg_{Pd+Pt}^{-1} after 2000 cycles	[4]
Pd_4Au_1P/CNT	1.0 M KOH and 1.0 M ethanol	2296	74.3	83.4 mA mg_{Pd}^{-1} after 7200 s	[5]
PdSnNi/CNT	1.0 M NaOH and 1.0 M ethanol	3.5	267	1.3 A/mg_{Pd} after 4000 s	[6]
PdCuP	1.0 M KOH and 1.0 M ethanol.	6670	69.2	NA	[7]
$Pd_{75}Cu_8Co_3$	1.0 M NaOH and 1.0 M ethanol	3948	57.0	4.2 A/mg_{Pd} after 10000 s	[8]
Au_2Cu@Pd	1.0 M KOH and 1.0 M ethanol.	2210	89.2	0.906 A/mg after 4 hours' test	[9]
$Cu_1Pd_1/Ir_{0.03}$ /NPGs	1.0 M KOH and 1.0 M ethanol	7105	75.96	51% after 500 cycle	[10]
Au@PdNi	1.0 M KOH and 1.0 M ethanol	5891	38.5	578 mA mg_{Pd}^{-1} after 3600s	[11]
$Pd_{31}Cu_{61}Co_8$	1.0 M KOH and 1.0 M ethanol	7450	88.3	6.77 A mg^{-1} after 100 cycle	[12]
PdRhTe NTs/C	1.0 M KOH and 1.0 M ethanol	2039	34.15	remained at 80.48% after 500 cycle	[13]
Pd_3NiP/N-rGO	1.0 M KOH and 1.0 M ethanol	2223	83.9	39 mA mg^{-1} after 6 h	[14]
PdCuB@N-G	1.0 M KOH and 1.0 M ethanol	5830	~83	3.62Amg^{-1} after 5000 cycles.	[15]
PdBP NWs@N-G	1.0 M KOH and 1.0 M ethanol	4150	~34	1870 mAmg_{Pd}^{-1} after 5000 cycles	[16]
PdRuCu	0.5 M KOH and 0.5 M ethanol	1160	30.78	4.08 mA cm^{-2} after 4000 s	[17]
c-Pd-Ni-P@a-Pd-Ni-P 170 °C	1.0 M KOH and 1.0 M ethanol.	3050	27 .5	0.38Amg_{Pd}^{-1} After 1800 s	[18]

Pd_7Ag	0.5 M KOH and 1.0 M ethanol	7080	49.6	2.35 A mg_{Pd}^{-1} after 3600s	[19]
Pd/AG-BP	1.0 M NaOH and 1.0 M ethanol	1972	276.98	712.03 mA mg_{Pd}^{-1} after at 20, 000 s	[20]
$Pt_{55}Pd38Bi_7$/RGO	1.0 M KOH and 1.0 M ethanol	14550 mA/mg_{Pd} 5410 mA/mg_{Pt}	136.6	54% of the initial value after 1000cycle	[21]
CoP/RGO-Pd10	1.0 M KOH and 1.0 M ethanol	4597	45.9	78.3% of its initial activity after 250 cycles	[22]
Pd_7Ag_3 NS/C	1.0 M KOH and 1.0 M ethanol	9365.9	97.6	111.0 mA mg_{Pd}^{-1} after 4,000s	[23]
9.0-nm-$Pd_{61}Pt_{22}Cu_{17}$ TNRs/C	1.0 M KOH and 1.0 M ethanol	12420 mA/$mg_{(Pd+pt)}$	93.7	NA	[24]
Pd/a-SrRuO	1.0 M KOH and 1.0 M ethanol	4000	77.29	570 mA mg_{Pd}^{-1} after 60000s	[25]
Ag@$Pd_2P_{0.2}$	1.0 M KOH and 1.0 M ethanol	7240	6.68	289 mA mg_{Pd}^{-1} after 7200s	[26]

NA: not available.

Reference

1. H. Lv, L. Sun, L. Zou, D. Xu, H. Yao and B. Liu, *Chem. Sci.*, 2019, **10**, 1986-1993.
2. H. Lv, L. Sun, X. Chen, D. Xu and B. Liu, *Green Chem.* 2019, **21**, 2043-2051.
3. T. Miao, Y. Song, C. Bi, H. Xia, D. Wang and X. Tao, *J. Phys. Chem. C*, 2015, **119**, 18434-18443.
4. H. Lv, L. Sun, D. Xu, S. L. Suib and B. Liu, *Green Chem.*, 2019, **21**, 2367-2374.
5. H. Yang, Z. Yu, S. Li, Q. Zhang, J. Jin and J. Ma, *J. Catal.*, 2017, **353**, 256-264.
6. L. Ning, X. Liu, M. Deng, Z. Huang, A. Zhu, Q. Zhang and Q. Liu, *Electrochim. Acta*, 2019, **297**, 206-214.
7. H. Lv, L. Sun, D. Xu, Y. Ma and B. Liu, *Appl. Catal. B: Environ.*, 2019, **253**, 271-277.
8. Y. Shu, X. Shi, Y. Ji, Y. Wen, X. Guo, Y. Ying, Y. Wu and H. Yang, *ACS Appl. Mater. Interfaces*, 2018, **10**, 4743-4749.
9. Q. Shi, C. Zhu, M. Tian, D. Su, M. Fu, M. H. Engelhard, I. Chowdhury, S. Feng, D. Du and Y. Lin, *Nano Energy*, 2018, **53**, 206-212.
10. L. Luo, C. Fu, F. Yang, X. Li, F. Jiang, Y. Guo, F. Zhu, L. Yang, S. Shen and J. Zhang, *ACS Catal.*, 2019, **10**, 1171-1184.
11. N. Sui, T. Wang, Q. Bai, R. Yue, H. Jiang, H. Xiao, M. Liu, L. Wang, Z. Zhu and W. W. Yu, *J. Alloy Comd.* 2020, **817**, 153335.
12. F. Zhao, C. Li, Q. Yuan, F. Yang, B. Luo, Z. Xie, X. Yang, Z. Zhou and X. Wang, *Nanoscale*, 2019, **11**, 19448-19454.
13. L. Jin, H. Xu, C. Chen, H. Shang, Y. Wang and Y. Du, *Inorg. Chem.*, 2019, **58**, 12377-12384.

14. S. R. Chowdhury, T. Maiyalagan, S. K. Bhattachraya and A. Gayen, *Electrochim. Acta*, 2020, **342**, 136028.
15. L. Sun, H. Lv, Y. Wang, D. Xu and B. Liu, *J. Phys. Chem. Lett.*, 2020, **11**, 6632-6639.
16. H. Lv, L. Sun, D. Xu and B. Liu, *Sci. Bull.*, 2020, **65**, 1823-1831.
17. R.-L. Zhang, J.-J. Duan, Z. Han, J.-J. Feng, H. Huang, Q.-L. Zhang and A.-J. Wang, *Appl. Surf. Sci.*, 2020, **506**, 144791.
18. P. F. Yin, M. Zhou, J. Chen, C. Tan, G. Liu, Q. Ma, Q. Yun, X. Zhang, H. Cheng, Q. Lu, B. Chen, Y. Chen, Z. Zhang, J. Huang, D. Hu, J. Wang, Q. Liu, Z. Luo, Z. Liu, Y. Ge, X. J. Wu, X. W. Du and H. Zhang, *Adv. Mater.*, 2020, **32**, 2000482.
19. F. Gao, Y. Zhang, F. Ren, Y. Shiraishi and Y. Du, *Adv. Funct. Mater.*, 2020, **30**, 2000255.
20. T. Wu, Y. Ma, Z. Qu, J. Fan, Q. Li, P. Shi, Q. Xu and Y. Min, *ACS Appl. Mater. Interfaces*, 2019, **11**, 5136-5145.
21. X.-T. Zhang, L.-N. Zhou, Y.-Y. Shen, H.-T. Liu and Y.-J. Li, *RSC Adv.*, 2016, **6**, 58336-58342.
22. M. Wang, R. Ding, Y. Xiao, H. Wang, L. Wang, C. M. Chen, Y. Mu, G. P. Wu and B. Lv, *ACS Appl. Mater. Interfaces*, 2020, **12**, 28903-28914.
23. X. Meng, Y. Ouyang, H. Wu, H. Huang, F. Wang, S. Wang, M. Jiang and L. Y. Zhang, *J. Colloid. Interface Sci.*, 2020, **586**, 200-207.
24. W. Wang, X. Zhang, Y. Zhang, X. Chen, J. Ye, J. Chen, Z. Lyu, X. Chen, Q. Kuang, S. Xie and Z. Xie, *Nano Lett.*, 2020, **20**, 5458-5464.
25. X. Wu, J. He, M. Zhang, Z. Liu, S. Zhang, Y. Zhao, T. Li, F. Zhang, Z. Peng, N. Cheng, J. Zhang, X. Wen, Y. Xie, H. Tian, L. Cao, L. Bi, Y. Du, H. Zhang, J. Cheng, X. An, Y. Lei, H. Shen, J. Gan, X. Zu, S. Li and L. Qiao, *Nano Energy*, 2020, **67**, 104247.
26. X. Yang, Z. Liang, S. Chen, M. Ma, Q. Wang, X. Tong, Q. Zhang, J. Ye, L. Gu and N. Yang, *Small*, 2020, **16**, 2004727.